Biochemical Pharmacology 77 (2009) 1531–1540

Contents lists available at ScienceDirect

Biochemical Pharmacology

journal homepage: www.elsevier.com/locate/biochempharm

Synthetic regulators of the 2-oxoglutarate oxidative decarboxylation alleviate the glutamate excitotoxicity in cerebellar granule neurons

Maria S. Kabysheva [a], Tatiana P. Storozhevykh [b], Vsevolod G. Pinelis [b], Victoria I. Bunik [a,*]

[a] Belozersky Institute of Physico-Chemical Biology, Lomonosov Moscow State University, 119992 Moscow, Russian Federation
[b] Research Center for Children's Health, Russian Academy of Medical Sciences, 119991 Moscow, Russian Federation

ARTICLE INFO

Article history:
Received 23 November 2008
Accepted 2 February 2009

Keywords:
Glutamate excitotoxicity
Calcium homeostasis
2-Oxoglutarate dehydrogenase
Phosphono analog of 2-oxoglutarate
Tricarboxylic acid cycle

ABSTRACT

Impairment of the 2-oxoglutarate oxidative decarboxylation by the 2-oxoglutarate dehydrogenase complex (OGDHC) is associated with the glutamate accumulation, ROS production and neuropathologies. We hypothesized that correct function of OGDHC under metabolic stress is essential to overcome the glutamate excitotoxic action on neurons. We show that synthetic phosphono analogs of 2-oxoglutarate, succinyl phosphonate and its phosphono ethyl ester, improve the catalysis by brain OGDHC through inhibiting the side reaction of irreversible inactivation of its first component, 2-oxoglutarate dehydrogenase. Under the substrate and cofactor saturation, the component and complex undergo the inactivation during catalysis with the apparent rate constant 0.2 min^{-1}. The inactivation rate is reduced by 90% and 60% in the presence of 50 μM succinyl phosphonate and its phosphono ethyl ester, correspondingly. In cultured cerebellar granule neurons exposed to excitotoxic glutamate, the phosphonates (100 μM) protect from the irreversible impairment of mitochondrial function and delayed calcium deregulation. The deregulation amplitude is decreased by succinyl phosphonate and its phosphono ethyl ester by 50% and 30%, correspondingly. Thus, succinyl phosphonate is more potent than its phosphono ethyl ester in protecting both the isolated brain OGDHC from inactivation and cultured neurons from the glutamate-induced calcium deregulation. The correlation of the relative efficiency of the phosphonates in vitro and in situ indicates that their cellular effects are due to targeting OGDHC, which is in accord with independent studies. We conclude that the compounds preserving the 2-oxoglutarate dehydrogenase activity are of neuroprotective value upon metabolic disbalance induced by glutamate excess.

1. Introduction

In humans, decreased activity of the mitochondrial multienzyme 2-oxoglutarate dehydrogenase complex (OGDHC) is associated with both the age-related [1] and inborn [2,3] neurological impairments. The complex includes multiple copies of the three catalytic components catalyzing a multistep process of the overall reaction (6) by the consecutive action of the 2-oxoglutarate dehydrogenase (E1o, EC 1.2.4.2), dihydrolipoyl succinyl transferase (E2o, EC 2.3.1.61) and dihydrolipoyl dehydrogenase (E3, EC 1.8.1.4).

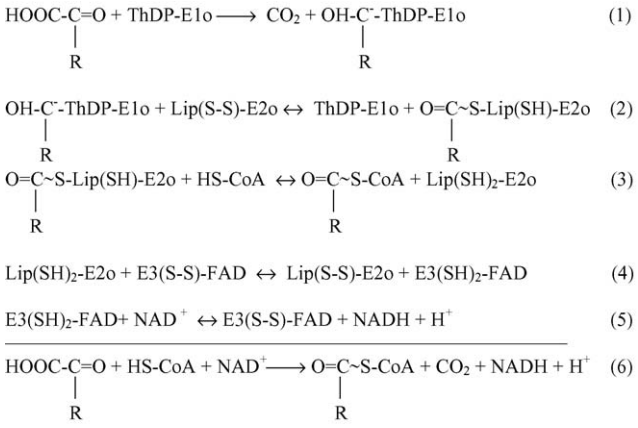

Among the mechanisms leading to the OGDHC inactivation under pathological conditions, the self-inactivation due to the side

* Corresponding author. Tel.: +7 495 939 44 84; fax: +7 495 939 31 81.
E-mail address: bunik@belozersky.msu.ru (V.I. Bunik).

Abbreviations: $[Ca^{2+}]_i$, intracellular concentration of calcium ions; NMDA, N-methyl-D-aspartate; OGDHC, 2-oxoglutarate dehydrogenase complex; ROS, reactive oxygen species; SP, succinyl phosphonate; $S_{0.5}$, the half-saturating concentration of a substrate; PESP, phosphonoethyl succinyl phosphonate.

0006-2952/$ – see front matter © 2009 Elsevier Inc. All rights reserved.
doi:10.1016/j.bcp.2009.02.001

reaction on the first and rate-limiting component of the complex, 2-oxoglutarate dehydrogenase, deserves special attention. This inactivation is a common feature of different OGDHC's [4,5], which accompanies the OGDHC-catalyzed ROS production [6] and is regulated by thioredoxin [5,7] and dicarboxylic acids [4]. Its regulatory significance for the OGDHC function within cellular network was suggested [7,8]. Analysis of available data indicated that metabolic disbalance under pathological conditions might stimulate the inactivation of OGDHC in the course of catalysis, leading to a vicious cycle of cellular impairment [9]. Therefore, we hypothesized that the compounds protecting brain OGDHC from the catalysis-associated inactivation could alleviate neuronal pathologies. The present work tests the hypothesis on the model of neuronal impairment due to the glutamate excitotoxicity. This model was chosen because of the inverse ratio between the OGDHC activity and glutamate concentration, which is an evolutionary conserved feature of metabolic networks [10–12]. Since glutamate is oxidized in the tricarboxylic acid cycle after the transamination to 2-oxoglutarate, reducing the OGDHC activity increases the glutamate concentration. In particular, we have recently shown that the OGDHC inhibition in situ leads to an increase in glutamate in heterotrophic plant tissues [11]. Extracellular glutamate also increased upon the OGDHC inhibition in rat brain [12]. These data suggest that accumulation of neurotoxic glutamate with decreasing the OGDHC activity underlies the known association of the OGDHC inactivation with neurological impairments [1–3]. Raising intracellular calcium, excitotoxic glutamate should increase both the concentration and oxidation of 2-oxoglutarate in mitochondria. This is anticipated because calcium not only activates the glutamate transport into neuronal mitochondria [13], where glutamate is in equilibrium with 2-oxoglutarate due to the transaminase reaction [14], but also increases the affinity of the 2-oxoglutarate dehydrogenase to 2-oxoglutarate [15]. In vitro, the increased concentration and oxidation of 2-oxoglutarate without an appropriate increase in the terminal OGDHC substrate, NAD^+, promote the production of ROS by the complex and the associated OGDHC inactivation [8,9]. In situ, significant contribution of OGDHC to the glutamate-induced increase in the neuronal ROS production has been recently shown [16]. Together, these data suggest that along with the OGDHC-dependent ROS production, the neuronal exposure to excitotoxic glutamate shall stimulate also the associated OGDHC inactivation. If so, protection of OGDHC from the inactivation during catalysis may help fighting neurodegeneration. Here, we introduce the synthetic phosphono analogs of 2-oxoglutarate as specific mechanism-based OGDHC inhibitors which, in particular, inhibit the OGDHC-catalyzed side reaction of self-inactivation. We further show their protective action on cerebellar granule neurons experiencing the glutamate insult. The insult is detected by the known effects of the excitotoxic glutamate on intracellular calcium and mitochondrial potential [17–19]. Relative efficiencies of the two phosphono analogs in vitro and in situ are shown to coincide, providing further evidence that it is the specific action of these mechanism-based inhibitors on cellular OGDHC that causes the observed changes in the integral cellular parameters. In conclusion, the mechanism of the neuroprotective effects of the phosphonates through their targeting of neuronal OGDHC is formulated.

2. Methods and materials

2.1. Reagents

The culture media (MEM, NBM), GlutaMax, B27, antibiotics were from "Gibco", USA; rhodamin 123 and acetoxymethyl ester of Fura-2FF were from "Molecular Probes", Netherlands, CoA was from "Gerbu", Germany. Succinyl phosphonate and its phosphono ethyl ester were synthesized and purified according to [20]. Other chemicals were from "Sigma", USA.

2.2. Brain OGDHC isolation and assay

The multienzyme complex was isolated from rat brain mitochondria according to [21]. The activities of the 2-oxoglutarate dehydrogenase component (reaction (1)) [22] and complex (reaction (6)) [20] were detected by hexacyanoferrate (III) and NAD^+ reduction, correspondingly, using saturating concentrations of all substrates. In particular, the 2-oxoglutarate dehydrogenase assay was done in 0.05 M potassium phosphate, pH 6.3, including 1 mM $MgCl_2$, 1 mM ThDP, 0.8 mM potassium hexacyanoferrate (III) and 0.1 mM 2-oxoglutarate (app. 5-fold $S_{0.5}^{OG}$ in the model system); the overall reaction was assayed in 0.1 M potassium phosphate, pH 7.0, containing 1 mM $MgCl_2$, 1 mM ThDP, 2.5 mM dithiothreitol, 1 mM 2-oxoglutarate (app. 10-fold $S_{0.5}^{OG}$), 0.1 mM CoA (app. 20-fold $S_{0.5}^{CoA}$), and 2.5 mM NAD^+ (app. 50-fold $S_{0.5}^{NAD}$). The initial (within 0.5 min of the reaction) rates were estimated in inhibition studies. The OGDHC preincubation with the phosphonates was done at a final dilution in the assay medium omitting substrates. To study protection by the analogs from the catalysis-induced inactivation of the 2-oxoglutarate dehydrogenase component and complex, the product accumulation curves were followed for 6 min and analyzed as in [23] using the bi-exponential approximations by SigmaPlot.

2.3. Cell cultures

Cerebellar granule cells were prepared from postnatal day 7–8 Wistar rat pups using standard procedure described earlier [24]. About 90% of cells in the culture were neurons, distinguished from glial cells by morphology and fluorescence change associated with calcium accumulation in response to glutamate.

2.4. Neuronal treatment with glutamate

Neuronal treatment with glutamate was done by incubation in the buffered salt solution, pH 7.4, without magnesium, containing, in mM: NaCl 135, KCl 5, glucose 5, $CaCl_2$ 1.8, HEPES 20, glycine 0.01, glutamate 0.1. At the end of the treatment, the neurons were washed out with the calcium-, glutamate- and glycine-free buffered salt solution, pH 7.4, containing, in mM: NaCl 135, KCl 5, glucose 5, $MgCl_2$ 2, HEPES 20, EGTA 0.1.

2.5. Simultaneous measurement of cytosolic calcium and mitochondrial potential in single neurons

Cellular indicators of cytosolic calcium (50 μg/ml acetoxymethyl ester of Fura-2FF) and mitochondrial potential (1 mg/ml Rh123) were dissolved in 30% DMSO and stored at −40 °C. Cells were loaded with 6 μM acetoxymethyl ester of Fura-2FF for 1 h in the presence of 0.001% Pluronic F127 in buffered salt solution, pH 7.4, containing, in mM: NaCl 135, KCl 5, glucose 5, $CaCl_2$ 1.8, $MgCl_2$ 1.0, HEPES 20. 3 μM Rh123 was added to the medium during the last 20 min of the Fura-2FF loading. SP or PESP were loaded simultaneously with Fura-2FF/Rh123 for 1 h, if not specified otherwise. After the loading was completed, cells were washed with the buffered salt solution omitting indicators and Pluronic.

A cell-coated glass was placed in a perfusion chamber (0.2 mL) mounted on the stage of an inverted epifluorescent microscope (Axiovert 200 "Zeiss", Germany) equipped with CCD camera (SnapCool-fx, USA). Fluorescence intensity was monitored every 20 s at room temperature (24–27 °C). The entire soma of individual neurons was used as region of interest. Kinetics of the fluorescence

changes was studied for the representative sample of neurons (about 40 cells) using Metafluor 6.1 software (Universal imaging corp., USA). Fluorescence images of the cells for Ca^{2+} were acquired at 505 nm emission (15 nm bandwidth) during alternate (in 100–200 ms pulses) excitation at 340 and 380 nm. The background fluorescence levels were determined at each wavelength and subtracted prior to calculating the ratio. Absolute values of $[Ca^{2+}]_i$ were determined using the Grynkiewicz equation [25] and the K_d value of 5 μM for Fura-2FF [26]. For calibration, the intracellular Fura-2FF saturation with calcium was achieved upon addition to the cell incubation medium of 5 μM ionomycin with 10 mM $CaCl_2$. Ca^{2+}-free buffer (1 mM EGTA) with 5 μM ionomycin was used to measure the fluorescence of free Fura-2FF in cells.

Rh123 was excited at 488 nm and emission was detected at 535 nm (10 nm bandwidth). Maximal values of the mitochondrial depolarization were determined as the fluorescence intensity after addition of 1 μM FCCP. The glutamate-induced changes of Rh123 were expressed as the percentage of this maximal depolarization after the FCCP addition.

2.6. Statistical analysis

Data are reported as means ± SEM. Statistical analysis was performed by the unpaired two-tailed Student's *t*-test using SigmaPlot Ver.10 Systat Software, Inc.

3. Results

3.1. Inhibition of brain OGDHC by phosphono analogs of 2-oxoglutarate is accompanied by their protection of OGDHC from the catalysis-associated inactivation

To study the action of the specific OGDHC inhibitors on the rat cerebellar granule cells, we first assessed in vitro effects of the compounds on OGDHC purified from rat brain. Fig. 1 shows inhibition by the phosphono analogs of 2-oxoglutarate of the initial rate of the overall reaction (6) catalyzed by the purified complex. After a preincubation of OGDHC with succinyl phosphonate (SP) or its phosphono ethyl ester (PESP) (Fig. 1A), 50% inhibition is achieved already with 5 μM phosphonates at 1 mM 2-oxoglutarate. The latter substrate concentration represents app. 10-fold excess over the half-saturating concentration for brain OGDHC [21]. The strong inhibition at such a high saturation of the complex with 2-oxoglutarate (Fig. 1) confirms the high efficiency of the phosphono analogs of 2-oxoglutarate, which was also observed in the inhibition studies of the 2-oxoglutarate dehydrogenase component and complex from other sources [20,27,28]. Kinetic study of the inhibition reveals several features of the interaction of the enzyme with the phosphono analogs. First of all, the inhibitory effect depends on the enzyme preincubation with the analogs. More obvious at a low (5 μM) concentrations or with PESP, an increase in the inhibition occurs, if prior to the substrate addition the inhibitors interacted with OGDHC in the medium without 2-oxoglutarate (Fig. 1A vs. B). Secondly, as expected for the closest structural analogs of the substrate, the inhibition of brain OGDHC by the phosphonates is competitive to 2-oxoglutarate. Since the interaction of brain OGDHC with both phosphonates (Fig. 1) and 2-oxoglutarate [21] is complex and does not follow the Michaelis kinetics, the competition was shown by comparing the inhibition of initial NADH production rates at 1 mM (app. 10-fold $S_{0.5}^{OG}$ [21]) and 0.1 mM (approx. $S_{0.5}^{OG}$ [21]) 2-oxoglutarate after the preincubation of OGDHC with a fixed (50 μM) SP concentration. Under these conditions, the residual activity was 30% at 1 mM 2-oxoglutarate, whereas no activity was detected at 0.1 mM 2-oxoglutarate. Thirdly, independent of preincubation, SP is a more efficient inhibitor than PESP (Fig. 1). For the half of the active sites the difference may be not obvious after preincubation with low (5 μM) concentrations (Fig. 1A), because under these conditions they are already saturated by either SP or PESP ($I_{50}^{SP,PESP} < 5$ μM). However, the other half of the active sites which is saturated at much higher concentrations of the inhibitors even after the preincubation, shows a higher affinity to SP (50 μM $< I_{50}^{SP} <$ 100 μM, Fig. 1A) compared to PESP ($I_{50}^{PESP} \gg 100$ μM, Fig. 1A). Without preincubation (Fig. 1B), neither the significant inhibition at low concentrations of the phosphonates, nor the half-of-the-sites reactivity are apparent, with all the active sites preferably targeted by SP (I_{50}^{SP} = 50 μM) compared to PESP ($I_{50}^{PESP} >$100 μM).

In addition to the inhibition of the initial NAD^+-reductase rates (Fig. 1), the analogs also affected the enzyme inactivation in the course of catalysis (Fig. 2), known to result in non-linear product accumulation kinetics [4,23]. As shown earlier for OGDHC from pigeon breast muscle and bovine heart, the enzymatic activity decreases in the course of catalysis due to the changes in the first rate-limiting component, 2-oxoglutarate dehydrogenase. This results in the biphasic product accumulation with similar kinetic parameters in the partial (reaction (1) in the presence of artificial electron acceptor hexacyanoferrate (III)) and overall (reaction (6)) 2-oxoglutarate dehydrogenase reactions [4]. Here, we show that the same feature is inherent in OGDHC from brain. As indicated by dashed curves in Fig. 2, both the full complex (Fig. 2A, hollow circles) and its 2-oxoglutarate dehydrogenase component (Fig. 2B, hollow circles) exhibit similar activity decays in the course of

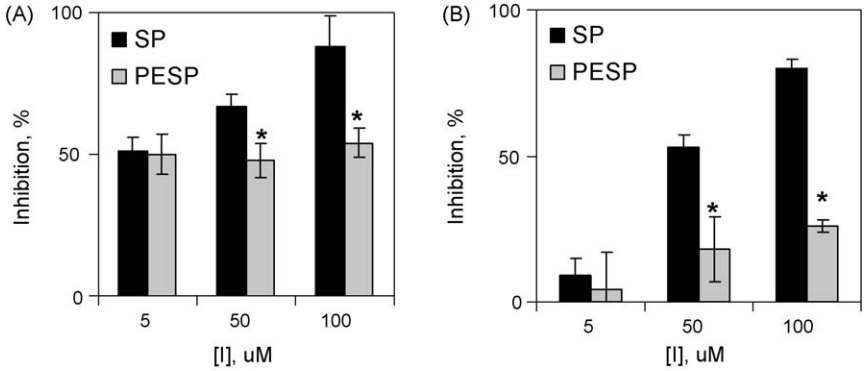

Fig. 1. Concentration dependence of the OGDHC inhibition by SP and PESP. Inhibition $(v_0 - v_i)/v_0$, %, was calculated from initial rates of the NADH production by purified brain OGDHC at the saturating concentrations of all substrates including 2-oxoglutarate (1 mM, approx. 10-fold $S_{0.5}^{OG}$ [21]). The enzyme was preincubated for 5 min with the analogs in the assay medium without substrates (A) or added to the complete reaction medium (B). Assay details are given in Section 2. Statistically significant differences between the SP and PESP action ($p \leq 0.05$) are marked by asterisks.

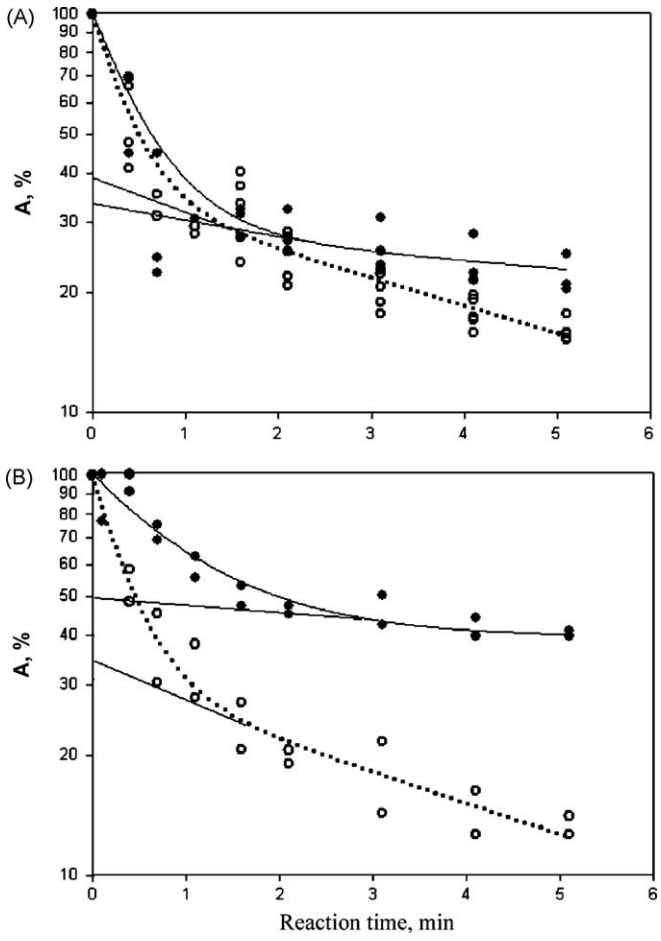

Fig. 2. Influence of SP on the decrease in the brain 2-oxoglutarate dehydrogenase activity (A, %) during the overall (A) and partial (B) 2-oxoglutarate dehydrogenase reactions. Superposition of two to four experimental curves (shown by the same symbols at a fixed reaction time) was used to approximate the dependence by a bi-exponential process [23] as described in Section 2. Linear extrapolation of the second phase to zero time shows the percentage of the activity lost during the first and second phases of the reaction. The control (dashed curves) and SP-affected (solid curves) values are represented by the hollow and filled circles, correspondingly. The overall reaction (6) (A) was followed by the NADH production at 1 mM 2-oxoglutarate and 5 μM SP, the partial reaction (1) (B) – by the hexacyanoferrate (IV) production at 0.1 mM 2-oxoglutarate and 0.5 μM SP.

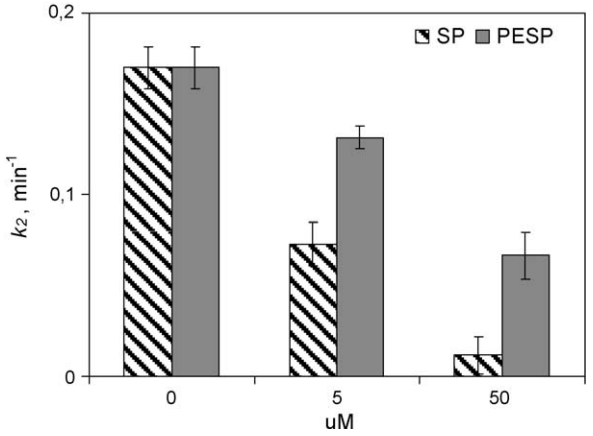

Fig. 3. Influence of SP and PESP on the rate of the catalysis-associated inactivation (k_2, min^{-1}) of brain OGDHC. The reaction was started by the substrate addition after 5 min preincubation of OGDHC with the inhibitors in the assay medium without substrates. The kinetic treatment of the activity decay was performed as in [23].

catalysis, confirming the role of the first component in the overall activity decay. In accord with the previous study [4], about 60–70% of the overall (reaction (6)) and partial (reaction (1)) activities are reversibly inhibited within several minutes from the reaction start, with the residual 30–40% of the activities undergoing irreversible decay (Fig. 2, dashed curves). The indicated percentage of the activity decrease during the first and second phase is determined from the linear extrapolation of the second phase to zero time as shown by lines in Fig. 2. The irreversible decay is characterized by an apparent rate constant k_2, min^{-1}, which is calculated from the semi-logarithmic plots (Fig. 2) as a slope of the second phase [4,23]. With the 2-oxoglutarate dehydrogenase component and complex from brain catalyzing the reactions at saturating 2-oxoglutarate, the irreversible inactivation occurred with the apparent rate constant of 0.2 min^{-1}. Phosphonates significantly slow down the activity decay during the second phase (Fig. 2, solid curves) in both the overall (Fig. 2A, filled circles) and partial (Fig. 2B, filled circles) reactions. The effect is concentration-dependent, with the stronger inhibitor SP being also a more efficient protector than PESP (Fig. 3). For example, at a fixed (50 μM) concentration of SP or PESP the apparent rate constant k_2 is reduced to 7% or 40% of the initial value, respectively (Fig. 3). Thus, inhibition of OGDHC by the phosphono analogs of 2-oxoglutarate is accompanied by their protection of the 2-oxoglutarate dehydrogenase from the catalysis-associated inactivation. Compared to PESP, SP is more efficient in both the inhibition and protection (Figs. 1, 3).

3.2. SP slows down the glutamate-induced calcium deregulation of cerebellar granule neurons in the time- and concentration-dependent manner

To detect possible influence of the 2-oxoglutarate phosphono analogs on neuronal responses to excitotoxic glutamate, we started with the more efficient effector of brain OGDHC, SP. Its action was examined in the established model of the glutamate excitotoxicity in cerebellar granule neurons [17–19]. In this model, glutamate induces an irreversible increase in intracellular calcium to abnormally high levels. This so called delayed calcium deregulation is detected by an increase in fluorescence of cells loaded with the calcium indicator Fura-2FF. The neurons in the microscope field may be distinguished by the false color scale of the fluorescence intensity. According to this scale, the highly fluorescent neurons, i.e. those having completed the glutamate-induced transition to the high intracellular calcium levels, are represented by red color, while those which have not, are colored green. Using this test, we estimated the neuronal calcium handling by calculating the percentage of the deregulated (red) neurons in the microscopic field at several fixed time points. Fig. 4 shows that increasing the time of pre-incubation of neurons with SP (from 5 to 60 min, Fig. 4A) or the SP concentration in the medium (from 20 to 100 μM, Fig. 4B) interfered with the transition of the neuronal sample to the high intracellular calcium levels. 60 min preincubation with 100 μM SP led to statistically significant decreases in the number of neurons undergoing the delayed calcium deregulation upon incubation with 100 μM glutamate over the entire observation time (Fig. 4, the points marked with asterisks). These optimized conditions were further employed in comparative studies of the SP and PESP action on single neurons.

3.3. Protection of the cerebellar granule neurons from the glutamate excitotoxicity by SP and PESP

The influence of the OGDHC inhibitors on the calcium homeostasis and mitochondrial potential of neurons affected by glutamate is shown in Figs. 5–7. Fig. 5A–C show kinetic traces of typical changes in intracellular calcium of single neurons

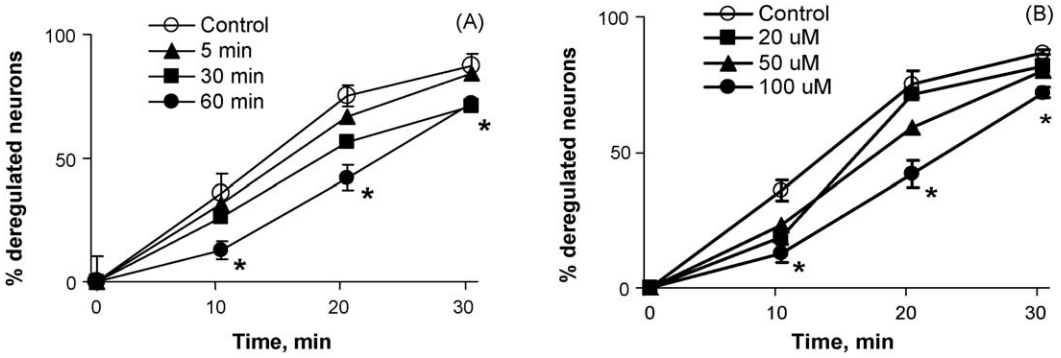

Fig. 4. Time (A) and concentration (B) dependencies of the SP influence on the delayed calcium deregulation induced by glutamate (100 μM) in cerebellar granule neurons. At the time points indicated, the percentage of the deregulated neurons in the microscopic field was determined by the false color fluorescence scale (see text for the details). Experimental details are given in Section 2.

detected by fluorescence of Fura-2FF upon prolonged incubation of cerebellar granule neurons with excitotoxic concentration (100 μM) of glutamate. Single traces of representative neurons are shown by black lines in Fig. 7. Under the experimental conditions, glutamate induces a rapid calcium influx through the NMDA receptors which is followed by a decrease in $[Ca^{2+}]_i$ (first peak in Figs. 5, 7) due to the mitochondrial calcium-buffering capacity [19,29]. After a latent period, the neurons undergo a further massive increase in $[Ca^{2+}]_i$ (Figs. 5, 7). At the same time, irreversible mitochondrial depolarization occurs (Fig. 6, grey lines in Fig. 7). Association of the two phenomena has been documented in a number of studies [19,29,30] and was also seen by us upon examining single neurons. As shown in Fig. 7, the changes in $[Ca^{2+}]_i$ and mitochondrial potential in each cell coincide in time, with both processes synchronously affected by the specific inhibitors of the mitochondrial OGDHC. The delayed calcium deregulation and accompanying changes in the mitochondrial potential induced by glutamate are irreversible, i.e. no restoration of the parameters is observed after removal of glutamate and calcium from the medium (Figs. 5A, 6A, and black lines in Figs. 5D, 6D). In the neurons loaded with SP or PESP no significant changes in the first transient calcium peak are observed, indicative of no effect of the phosphonates on the glutamate signaling through the NMDA receptors. However, the adverse effects of glutamate are significantly less pronounced in the phosphonate-loaded neurons (Figs. 5–7). Regarding the calcium homeostasis, such cells are characterized by a slower development of the delayed calcium deregulation, with their transition leveling off at a significantly lower $[Ca^{2+}]_i$ concentrations (Fig. 5). In addition to the main transition, a slower phase after 1000 s could be revealed in the control and SP-treated neurons (Fig. 5D, the black and dark grey curves). Analysis of the distribution of the traces of single neurons (Fig. 5A,B) indicates that this slower phase is due to a minor part of the cells undergoing the transition, mostly to a higher calcium levels, at a later time. Sub-populations of cerebellar granule cells regarding the glutamate excitotoxicity were also distinguished in other studies [30,31]. Unlike the control or SP-loaded cells, the PESP-loaded cells did not exhibit a distinct differentiation into the sub-populations

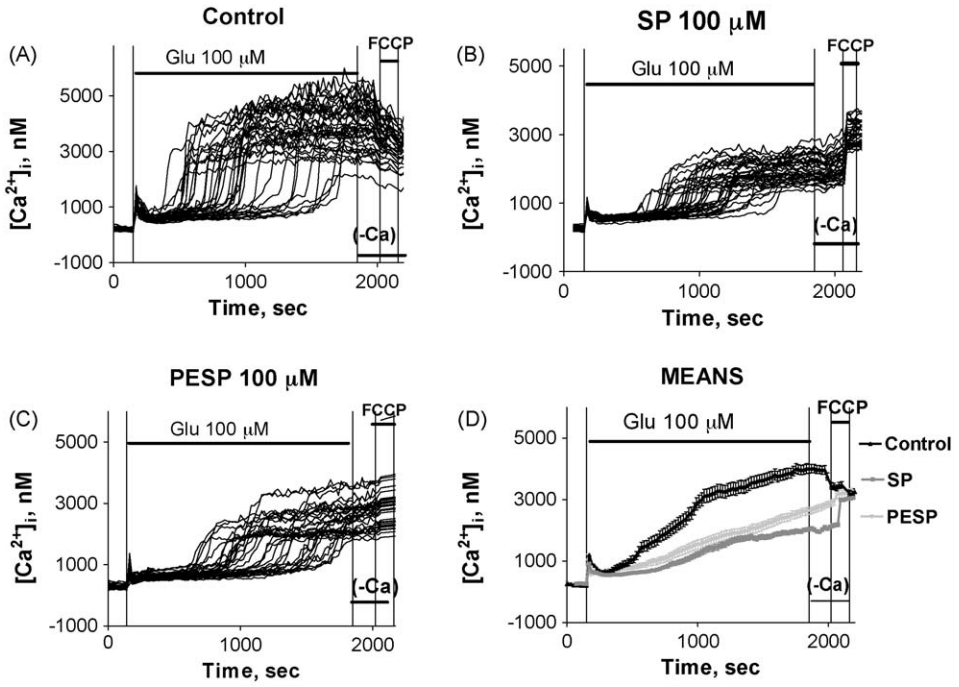

Fig. 5. Changes in the intracellular calcium, $[Ca^{2+}]_i$, of cerebellar granule neurons exposed to the prolonged action of glutamate (100 μM) alone (A) or in the presence of 100 μM SP (B) or PESP (C). Cells were preincubated with the analogs for one hour before the glutamate addition. In (D), the mean transitions of the neuronal cell samples shown in (A–C) are presented by black line (glutamate alone, $n = 43$), dark grey line (glutamate with SP, $n = 38$) and light grey line (glutamate with PESP, $n = 38$). Experimental details are given in Section 2.

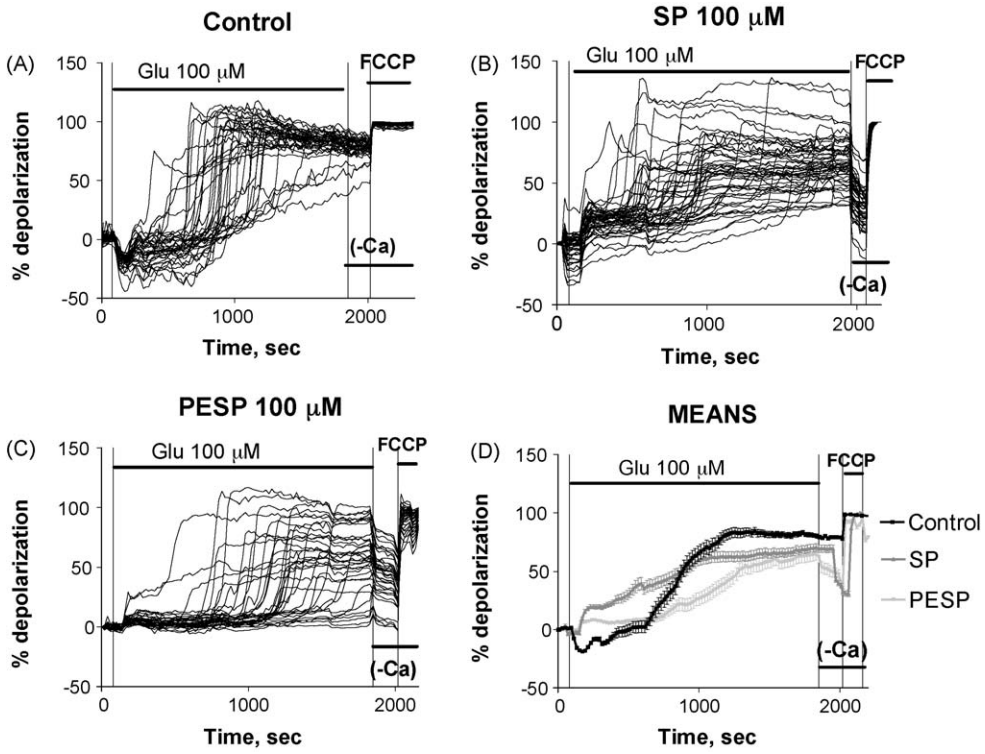

Fig. 6. Changes in the mitochondrial potential of cerebellar granule neurons exposed to the prolonged action of glutamate (100 μM) alone (A) or in the presence of 100 μM SP (B) or PESP (C). Cells were preincubated with the analogs for 1 h before the glutamate addition. In (D), the mean transitions of the neuronal cell samples shown in (A–C) are presented by black line (glutamate alone, $n = 43$), dark grey line (glutamate with SP, $n = 38$) and light grey line (glutamate with PESP, $n = 38$). Experimental details are given in Section 2.

(Fig. 5A–C), generally showing less synchronicity in the transition. More variety in the transition start and/or calcium increase amplitude resulted in the monotonous calcium transition kinetics of the PESP-loaded neuronal sample, in contrast to the biphasic kinetics inherent in the control and SP-loaded cells (Fig. 5D).

Concomitant with the changes in the onset time and amplitude of the calcium transition (Fig. 5), the neurons loaded with the phosphonates show different kinetics of the mitochondrial depolarization (Fig. 6). The mean traces (Fig. 6D) indicate that the bulk depolarization occurred within 500 s in the control cells (from app. 700 to 1200 s of the incubation with glutamate), whereas in the SP and PESP-loaded cells it required 900 s and more, respectively. In addition to the slower bulk depolarization, significant reversibility of the depolarization was observed in the phosphonate-loaded cells. That is, after removal of glutamate and calcium from the medium they exhibited a decrease in Rh123 fluorescence, not observed in the control cells (Fig. 6). The reversibility was also obvious from the amplitude of the following response to uncoupler. That is, the FCCP-induced increase in the Rh123 fluorescence was significantly (2–3-fold) higher in the phosphonate-loaded cells than in the control ones (Fig. 6D). Thus, in neurons exposed to excitotoxic glutamate concentration the phosphonates protect mitochondria from irreversible loss of function, which coincides with improved calcium handling.

3.4. SP has a higher neuroprotective potency than PESP

Quantitative differences of the SP and PESP action on the neuronal impairment induced by glutamate were analyzed by comparing their protection from the delayed calcium deregulation. As seen from Fig. 5B, the SP-loaded neurons finish the transition at 1400–2700 nM $[Ca^{2+}]_i$, whereas the PESP-loaded neurons increase their $[Ca^{2+}]_i$ to higher levels (2200–3500 nM, Fig. 5C). Nevertheless, the latter values of $[Ca^{2+}]_i$ are lower compared to the control cells, where the transition is finished at 2500–5000 nM (Fig. 5A). The average concentrations of the intracellular calcium after the glutamate-induced deregulation approached 4000, 2000 and 2800 nM $[Ca^{2+}]_i$ in the control, SP- and PESP-loaded neurons, respectively (Fig. 5D). Thus, at a fixed concentration (100 μM) and preincubation time (60 min) PESP shows a lower potency, preventing the neuronal $[Ca^{2+}]_i$ increase by 30% compared to 50% protection by SP (Fig. 5D). This conclusion was supported by analyzing kinetics of the transition from the mean traces (such as in Fig. 5D) of at least three independent experiments. Normalized to the maximal amplitude of the $[Ca^{2+}]_i$ increase at the end of experiment, such curves showed a good coincidence, enabling comparison of several kinetic parameters. These parameters were determined for the main transition, i.e. the slower phase which could be observed in the control and SP-loaded neurons (see above) was not characterized kinetically due to its small and variable contribution to the overall transition. The kinetics of the delayed calcium deregulation was characterized by the mean lag-period before the transition onset; the maximal rate of $[Ca^{2+}]_i$ increase in the neuronal population, and the mean time of the transition end. Table 1 shows that SP reliably increased the lag-period without significant changes in the rate and final time of the transition. PESP was more affecting the maximal rate of the

Table 1
Quantitative differences in the SP and PESP protection from the glutamate-induced delayed calcium deregulation.

Cell treatment	Lag-period (s)	Transition rate (%/s)	Time of the transition end (s)
Control	190 ± 100	0.080 ± 0.016	1270 ± 220
SP (100 μM)	530 ± 210*	0.075 ± 0.020	1560 ± 150
PESP (100 μM)	380 ± 100	0.055 ± 0.005*	1720 ± 130*

Statistically significant differences ($p \leq 0.05$) are marked by asterisks.

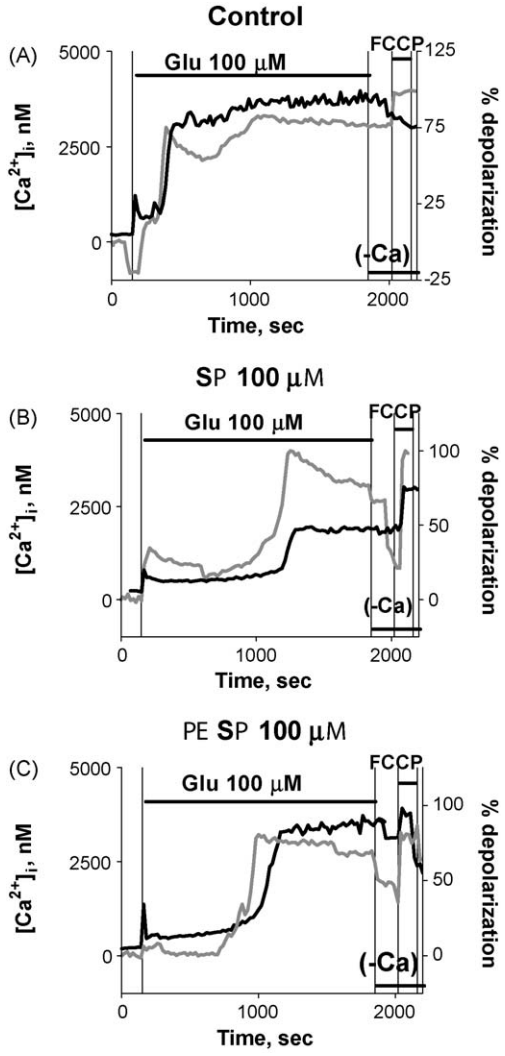

Fig. 7. Intracellular calcium $[Ca^{2+}]_i$ (black line) and mitochondrial potential (grey line) of single cerebellar granule neurons exposed to the prolonged action of excitotoxic concentration of glutamate (100 μM) after 1 h preincubation of the cells without (A) or with 100 μM SP (B) or PESP (C). Experimental details are given in Section 2.

transition, delaying the time of the transition end. Thus, there were statistically significant quantitative differences in the SP and PESP protection from the delayed calcium deregulation (Fig. 5D, Table 1).

Although both the changes in Rh123 fluorescence and the process of mitochondrial depolarization are too complex to be characterized quantitatively, some differences in the effects of SP and PESP on mitochondrial potential were also notable (Fig. 6D). In the SP-loaded neurons the mitochondrial depolarization after the glutamate addition was more pronounced than in the PESP-loaded neurons. That is, in the SP-loaded neurons the glutamate-induced depolarization started right after the glutamate addition, and by 600 s of the treatment SP already induced about 40% of the maximal depolarization. The PESP-loaded neurons only started their depolarization by that time, and the delay did not differ from that in the control experiment where glutamate induced the mitochondrial depolarization without the phosphonates (Fig. 6D).

As a result, the PESP-loaded neurons showed no significant changes in the onset of either the delayed calcium deregulation (Table 1) or bulk mitochondrial depolarization (Fig. 6D). In contrast, the more rapid depolarization of the mitochondria of the SP- vs. PESP-loaded neurons (Fig. 6D) was accompanied by the delayed onset of the calcium deregulation (Fig. 5D, Table 1) and a higher reversibility of the depolarization process after removal of glutamate and calcium from the medium (Fig. 6D). Thus, the more rapid depolarization in the presence of a stronger OGDHC inhibitor SP provided for a better preservation of the mitochondrial function (Fig. 6D) and calcium homeostasis (Fig. 5D) upon the glutamate insult.

4. Discussion

4.1. Mechanism of interaction of SP and PESP with brain OGDHC provides for efficient and specific inhibition protecting from the catalysis-associated inactivation

Phosphono analogs of 2-oxoglutarate have received increasing attention as promising tools for inhibition of OGDHC in native cells and tissues [11,14,16,20]. To better understand their action in the neuronal culture, we characterized their effects on the purified brain OGDHC at the 2-oxoglutarate concentrations known to occur inside mitochondria ($10^{-4} - 10^{-3}$ M, [8]). Our study showed that under these conditions the phosphonates efficiently compete with 2-oxoglutarate at the active site of the 2-oxoglutarate dehydrogenase component of brain OGDHC, with the inhibition occurring according to the slow tight binding mechanism. The kinetically slow conformational transition of the initial enzyme-inhibitor complex to a tightly bound inhibitor complex represents a general property of the ternary complexes of the 2-oxo acid dehydrogenases with the coenzyme thiamine diphosphate and phosphono analogs of their respective substrates [11,32–34]. In these complexes, the phosphonates are bound much stronger than in other enzymes due to formation of the transition state analogs [20,27,35–37], with the tight binding and highly specific formation of the latter especially attractive for cellular studies. Esterification of the phosphono group of SP (methylation used earlier [27,28] or ethylation used in the present work and with plant OGDHC [11]) significantly decreases efficiency of the OGDHC inhibition. This is in contrast to the pyruvate dehydrogenase which reacts more readily with the methyl ester of the pyruvate phosphono analog [35,36]. Together with the strongly varied efficiency of the phosphonate inhibition of different classes of the thiamine diphosphate-dependent enzymes [37], the difference in the structural requirements of the pyruvate and 2-oxoglutarate dehydrogenases to the respective phosphonate structures stresses the importance of the specific catalysis-associated interactions for the formation of the tightly-bound complexes even within the same enzyme class. Thus, the mechanism of the inhibition of OGDHC by the phosphono analogs of 2-oxoglutarate provides for the high selectivity and efficiency of the interaction.

The thiamine-diphosphate dependent enzymes are known to exhibit the half-of-the-sites reactivity to their substrates, with alternative conformations of the two active sites in a functional dimer representing different steps along the reaction coordinate at each given moment of time [38–42]. In particular, formation of the covalent adduct with ThDP only in one of the active sites was shown to occur upon interaction of the 2-oxoglutarate dehydrogenase with 2-oxoglutarate [38] and for the yeast pyruvate decarboxylase binding methyl acetylphosphonate [42]. The pre-incubation-induced difference in the reactivities of the 50% active sites to the phosphonates (Fig. 1) may thus be explained by different stabilization of the covalent adduct of the phosphonates with ThDP in the two active sites of the brain 2-oxoglutarate dehydrogenase dimer.

Along with the OGDHC inhibition, the phosphono analogs of the substrate are shown here to efficiently protect brain OGDHC from the irreversible inactivation of the 2-oxoglutarate dehydrogenase component during catalysis (Figs. 2, 3). The self-inactivation of

enzymes producing highly active compounds is a feasible means to stop production of such compounds already at their very low concentrations [43,44]. At least two of the highly reactive intermediates are generated within OGDHC: the thiyl radical of the complex-bound lipoyl residue and the carbon radical of the enamine intermediate at the active site of the 2-oxoglutarate dehydrogenase [6,45]. The accompanying OGDHC inactivation is slowed down, in particular, by the natural 2-oxoglutarate structural analogs [4]. Whereas the most efficient from these natural protectors, malonate, caused only 40% protection at 3 mM, SP in our experiments with the brain complex caused more than 50% protection already at a three orders of magnitude lower concentration (5 μM, Fig. 3). The powerful preservation of the brain OGDHC activity by the phosphonates (Figs. 2, 3) correlates with their inhibition of the OGDHC-dependent ROS production [16], the process inducing the enzyme inactivation [6,8]. Both effects of the phosphonates are of potential neuroprotective value, as the metabolic disbalance under pathological conditions is supposed to stimulate both the OGDHC-dependent ROS production and associated inactivation, with the latter being among the potential causes of the neurodegenerative diseases [9].

4.2. Correlation of the neuronal protection by the phosphono analogs of 2-oxoglutarate with their effects on OGDHC

In a native cell the concentrations of the OGDHC substrates and inhibitors determining the OGDHC activity depend on multiple systems and fluxes, which cannot be imitated in vitro for the OGDHC activity estimations. Existing approaches do not allow for a simultaneous determination of the intracellular OGDHC activity and integral parameters of native cells under certain experimental conditions. However, as shown above, the phosphonate analogs of 2-oxoglutarate are highly specific mechanism-based inhibitors of OGDHC. Selective action of the phosphonates on OGDHC in cellular studies is further supported by similar relative efficiency of SP and PESP in their action on cells and on OGDHC. Possessing a lower affinity (Fig. 1) and less efficient in the protection of OGDHC from the catalysis-associated inactivation (Fig. 3), PESP is also less active in situ. That is, the PESP-loaded cells are less resistant to the delayed calcium deregulation and mitochondrial impairment than the SP-loaded neurons (Figs. 5D, 6D, Table 1). Remarkably, the neuronal functions are better preserved by a stronger OGDHC inhibitor and protector SP (Figs. 1, 3), which also shows no delay in the depolarizaton of mitochondria compared to PESP (Fig. 6D). A stronger depolarization of the glutamate-affected mitochondria by SP compared to its ester was also shown for hippocampal neurons [16]. The phosphonate-induced depolarization obviously opposes the primary action of glutamate which is known to hyperpolarize mitochondria before inducing the irreversible loss of function in both the hippocampal [16,46] and cerebellar granule neurons [31]. Thus, the reversible mitochondrial depolarization due to the OGDHC inhibition by the phosphonates may prevent the mitochondrial overreaction to the glutamate insult, alleviating damaging consequences of the glutamate action.

Along with the observed correspondence in the SP and PESP efficiencies in situ (Figs. 5D, 6D, Table 1) and in vitro (Figs. 1, 3), dependence of their cellular action on the OGDHC targeting is further supported by no significant interaction of the phosphonates with a number of enzymes transforming 2-oxoglutarate or its natural structural analogs [11,20]. Besides, cellular experiments with labeled compounds, metabolomic studies and examination of the particularly related to the OGDHC reaction amino acid pools [11,14] showed that the phosphonates caused the changes in the label distribution and tissue metabolites, which are anticipated to occur due to the OGDHC inhibition. Furthermore, a strong reduction in the mitochondrial respiration [11] and potential

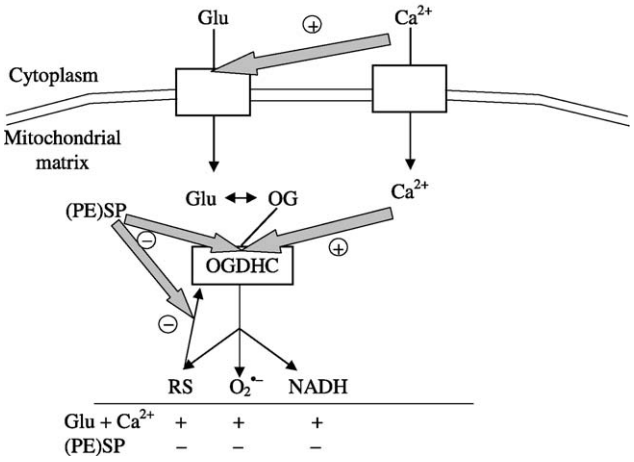

Fig. 8. Mechanism of the neuroprotective action of the phosphono analogs of 2-oxoglutarate. The transport and catalytic processes under consideration are indicated by the thin black arrows. The negative influence on the OGDHC activity of the reactive species (RS)-involving reaction is shown by (−). The bold grey arrows show regulatory effects of calcium and phosphonates, increasing (+) or decreasing (−) the processes to which the arrows point. The net effects of glutamate with calcium (Glu+Ca^{2+}) or phosphonates upon the glutamate stimulation ((PE)SP) are summarized below the line. See text for other details.

[16] by the phosphonates was shown, in accord with the OGDHC inhibition by the phosphonates controlling these integral parameters of mitochondrial function.

4.3. Mechanism of the neuroprotective action of the phosphono analogs of 2-oxoglutarate under the glutamate excitotoxicity

Fig. 8 shows the OGDHC-related events in neurons stimulated by glutamate. The signaling action of extracellular glutamate increases intracellular calcium. At the same time the glutamate may be used for oxidation in neuronal mitochondria where glutamate is transaminated to 2-oxoglutarate [14]. Cytoplasmic calcium is known to activate the glutamate transport into neuronal mitochondria [13]. Mitochondrial accumulation of calcium increases the efficiency of the glutamate oxidation by increasing the affinity of OGDHC to 2-oxoglutarate [15]. As a result, the neuronal flux through OGDHC should be increased in the presence of glutamate, leading to increased NADH and ROS production by OGDHC. The OGDHC-dependent increase in NADH may explain the initial hyperpolarization of mitochondria in response to the glutamate addition [16,31,47], which was shown to be blocked by the phosphonates [16]. Contribution of the OGDHC-dependent ROS to those produced by neurons overstimulated with glutamate was also shown [16]. The OGDHC-bound reactive species (RS, Fig. 8), such as thiyl radical of the OGDHC-bound lipoic acid and carbon-centered radical of the thiamine diphosphate-enamine adduct [6,45], are generated concomitant with the OGDHC-dependent ROS production. They should therefore increase in the presence of glutamate, leading to the increased rate of the OGDHC irreversible inactivation. Obviously, the neuronal resources to compensate for the inactivation of a key mitochondrial enzyme system are limited, and increasing the OGDHC inactivation upon prolongation of the glutamate action contributes to the glutamate excitotoxic effects, such as mitochondrial disfunction, disturbance in calcium homeostasis and metabolic stress.

Regarding the OGDHC-depedent events, the phosphono analogs of 2-oxoglutarate act as calcium antagonists. That is, by competing with 2-oxoglutarate at the active site of 2-oxoglutarate dehydrogenase, they decrease the calcium-increased efficiency of the 2-oxoglutarate binding (Fig. 8). As a result, they decrease the

OGDHC-dependent NADH production (Fig. 1), mitochondrial potential [16], the OGDHC-generated ROS [16] and associated irreversible inactivation of OGDHC (Fig. 3). Because the inactivation of OGDHC accompanying neurodegenerative diseases was suggested to be among the causes of pathologies, progressively increasing due to metabolic stress [1,9], preservation of the OGDHC activity by the phosphonates provides for a plausible mechanism of their neuroprotective action revealed by us as improved calcium handling (Fig. 5, Table 1) and preserved mitochondrial function (Fig. 6) upon the glutamate insult. However, the question arises why the decrease in the OGDHC activity due to the inhibition of cellular OGDHC by the phosphonates does not negatively affect the neurons? Obviously, one should distinguish the consequences of the phosphonate action under normal and pathological conditions. In the former case, their application may model metabolic changes in the neurodegenerative diseases which are characterized by the decreased OGDHC activity. However, application of the phosphonates under the metabolic stress induced by neuronal overstimulation with glutamate brings to the first plan their protective action (Fig. 8). Furthermore, unlike the irreversible inactivation in the course of catalysis, the OGDHC inhibition by the phosphonates may be self-regulated, with the accumulated intramitochondrial 2-oxoglutarate acting as a positive effector restoring the OGDHC activity. The phosphonates may thus perform a buffering function, correcting the metabolic disbalance which arises upon increased flux through OGDHC in the presence of glutamate. Finally, dependent on conditions, cells may exhibit a significant spare threshold of the OGDHC activity, i.e. OGDHC may be partly inhibited without affecting the mitochondrial physiology [47]. Thus, inside neuronal mitochondria experiencing glutamate insult in the presence of the neuroprotective concentrations of the phosphonates (100 μM), the level of the phosphonate-induced inhibition of the physiological OGDHC reaction (reaction (6)) may be within the spare treshold, and/or adjustable according to the concentration of the OGDHC substrates. In contrast, concomitant inhibition by the phosphonates of the OGDHC-dependent side-reactions, such as production of ROS and intrinsic reactive species leading to the irreversible OGDHC inactivation (RS), is neuroprotective (Fig. 8).

Acknowledgements

We are grateful to Prof. N.K. Lukashev and Dr. A.V. Kazantsev from the Chemistry Department of Moscow Lomonosov State University for synthesis and purification of the phosphono analogs of 2-oxoglutarate. Technical assistance of Mr. E.I. Klimuk with the OGDHC assays is acknowledged. The work was supported by grant 06-08-01441 from Russian Foundation of Basic Research.

References

[1] Gibson GE, Blass JP, Beal MF, Bunik V. The α-ketoglutarate dehydrogenase complex: a mediator between mitochondria and oxidative stress in neurodegeneration. Mol Neurobiol 2005;31:43–63.
[2] Dunckelmann RJ, Ebinger F, Schulze A, Wanders RJA, Rating D, Mayatepek E. 2-Ketoglutarate dehydrogenase deficiency with intermittent 2-ketoglutaric aciduria. Neuropediatrics 2000;31:35–8.
[3] Guffon N, Lopez-Mediavilla C, Dumoulin R, Mousson B, Godinot C, Carrier H, et al. 2-Ketoglutarate dehydrogenase deficiency, a rare cause of primary hyperlactataemia: report of a new case. Inherit Metab Dis 1993;16:821–30.
[4] Bunik VI, Pavlova OG. Inactivation of alpha-ketoglutarate dehydrogenase during its enzymatic reaction. Biochemistry (Moscow) 1997;62:973–82.
[5] Raddatz G, Kruft V, Bunik V. Structural determinants for the efficient and specific interaction of thioredoxin with 2-oxoacid dehydrogenase complexes. Appl Biochem Biotechnol 2000;88:77–96.
[6] Bunik V, Sievers C. Inactivation of the 2-oxo acid dehydrogenase complexes upon generation of intrinsic radical species. Eur J Biochem 2002;269:5004–15.
[7] Bunik V. Increased catalytic performance of the 2-oxoacid dehydrogenase complexes in the presence of thioredoxin, a thiol-disulfide oxidoreductase. J Mol Catal B Enzy 2000;8:165–74.
[8] Bunik V. 2-Oxo acid dehydrogenase complexes in redox regulation. Role of the lipoate residues and thioredoxin. Eur J Biochem 2003;270:1036–42.
[9] Bunik V, Schloss JV, Pinto JT, Gibson GE, Cooper AJL. Enzyme-catalyzed side reactions with molecular oxygen may contribute to cell signaling and neurodegenerative diseases. Neurochem Res 2007;32:871–91.
[10] Schultz C, Niebisch A, Gebel L. Glutamate production by Corynebacterium glutamicum: dependence on the oxoglutarate dehydrogenase inhibitor protein OdhI and protein kinase PknG. Appl Microbiol Biotechnol 2007;76:691–700.
[11] Araujo WL, Nunes-Nesi A, Trenkamp S, Bunik VI, Fernie AR. Inhibition of 2-oxoglutarate dehydrogenase in potato tuber suggests the enzyme is limiting for respiration and confirms its importance in nitrogen assimilation. Plant Physiol 2008;148:1782–96.
[12] Hazell AS, Butterworth RF, Hakim AM. Cerebral vulnerability is associated with selective increase in extracellular glutamate concentration in experimental thiamine deficiency. J Neurochem 1993;61:1155–8.
[13] Pardo B, Contreras L, Serrano A, Ramos M, Kobayashi K, Lijima M, et al. Essential role of Aralar in the transduction of small Ca^{2+} signals to neuronal mitochondria. Biol Chem 2006;281:1039–47.
[14] Santos SS, Gibson GG, Cooper AJL, Denton TT, Thompson CM, Bunik VI, et al. Inhibitors of α-ketoglutarate dehydrogenase complex alter [1-13C]glucose and [U-13C]glutamate metabolism in cerebellar granule neurons. Neurosci Res 2006;83:450–8.
[15] Lawlis VB, Roche TE. Regulation of bovine kidney α-ketoglutarate dehydrogenase complex by calcium ion and adenine nucleotides. Effects on S0. 5 for α-ketoglutarate. Biochemistry 1981;20:2512–8.
[16] Zündorf G, Kahlert S, Bunik VI, Reiser G. alpha-Ketoglutarate dehydrogenase contributes to production of reactive oxygen species in glutamate-stimulated hippocampal neurons in situ. Neuroscience 2009;158:610–6.
[17] Budd SL, Nicholls DG. Mitochondria, calcium regulation and acute glutamate excitotoxicity in cultured cerebellar granule cells. J Neurochem 1996;67:2282–91.
[18] Nicholls DG, Vesce S, Kirk L, Chalmers S. Interactions between mitochondrial bioenergetics and cytoplasmic calcium in cultured cerebellar granule cells. Cell Calcium 2003;34:407–24.
[19] Khodorov BI. Glutamate-induced deregulation of calcium homeostasis and mitochondrial dysfunction in mammalian central neurones. Prog Biophys Mol Biol 2004;86:279–351.
[20] Bunik V, Denton TT, Xu H, Thompson CM, Cooper AJL, Gibson GE. Phosphonate analogs of α-ketoglutarate inhibit the activity of the α-ketoglutarate dehydrogenase complex isolated from brain and in cultured cells. Biochemistry 2005;44:10552–61.
[21] Bunik V, Kaehne T, Degtyarev D, Shcherbakova T, Reiser G. Novel isoenzyme of 2-oxoglutarate dehydrogenase is identified in brain, but not in heart. FEBS J 2008;275:4990–5006.
[22] Bunik VI, Raddatz G, Wanders R, Reiser G. Brain pyruvate and 2-oxoglutarate dehydrogenase complexes are mitochondrial targets of the CoA ester of the Refsum disease marker phytanic acid. FEBS Lett 2006;580:3551–7.
[23] Bunik VI, Romash OG, Gomazkova VS. Effect of alpha-ketoglutarate and its structural analogues on hysteretic properties of alpha-ketoglutarate dehydrogenase. FEBS Lett 1991;278:147–50.
[24] Khodorov BI, Storozhevykh TP, Surin AM, Iuriavichus AI, Sorokina EG, Borodin AV, et al. The leading role of mitochondrial depolarization in the mechanism of glutamate-induced disorder in Ca(2+)-homeostasis. Ross Fiziol Zh Im I M Sechenova 2001;87:459–67.
[25] Grynkiewicz G, Poenie M, Tsien RY. A new generation of Ca2+ indicators with greatly improved fluorescence properties. J Biol Chem 1985;260:3440–50.
[26] Golovina VA, Blaustein MP. Spatially and functionally distinct Ca2+ stores in sarcoplasmic and endoplasmic reticulum. Science 1997;275:1643–8.
[27] Bunik VI, Biryukov AI, Zhukov YuN. Inhibition of pigeon breast muscle α-ketoglutarate dehydrogenase by phosphonate analogues of α-ketoglutarate. FEBS Lett 1992;303:197–201.
[28] Biryukov AI, Bunik VI, Zhukov YN, Khurs EN, Khomutov RM. Succinyl phosphonate inhibits alpha-ketoglutarate oxidative decarboxylation, catalyzed by alpha-ketoglutarate dehydrogenase complexes from *E. coli* and pigeon breast muscle. FEBS Lett 1996;382:167–70.
[29] Nicholls DG, Budd SL. Mitochondrial and neuronal survival. Physiol Rev 2000;80:315–60.
[30] Ward MW, Rego AC, Frenguelli BG, Nicholls DG. Mitochondrial membrane potential and glutamate excitotoxicity in cultured cerebellar granule cells. Neurosci 2000;20:7208–19.
[31] Ward MW, Huber HJ, Weisova P, Dussmann H, Nicholls DG, Prehn JH. Mitochondrial and plasma membrane potential of cultured cerebellar neurons during glutamate-induced necrosis, apoptosis, and tolerance. Neurosci 2007;27:8238–49.
[32] Laber B, Amrhein N. Metabolism of 1-aminoethylphosphinate generates acetylphosphinate, a potent inhibitor of pyruvate dehydrogenase. Biochemistry 1987;248:351–8.
[33] Schönbrunn-Hanebeck E, Laber B, Amrhein N. Slow-binding inhibition of the *E. coli* pyruvate dehydrogenase multienzyme complex by acetylphosphinate. Biochemistry 1990;29:4880–5.
[34] Dixon HB, Giddens RA, Harrison RA, Henderson CE, Norris WE, Parker DM, et al. A synthesis of acylphosphonic acids and of 1-aminoalkylphosphonic acids: the action of pyruvate dehydrogenase and lactate dehydrogenase on acetylphosphonic acid. Enzyme Inhib 1991;5:111–211.

[35] Kluger R, Pike DC. Active site generated analogues of reactive intermediates in enzymic reactions. Potent inhibition of pyruvate dehydrogenase by a phosphonate analogue of pyruvate. Am Chem Soc 1977;99: 4504–6.
[36] Kluger R, Pike DC. Chemical synthesis of a proposed enzyme-generated "reactive intermediate analogue" derived from thiamin diphosphate. Self-activation of pyruvate dehydrogenase by conversion of the analogue to its components. Am Chem Soc 1979;101:6425–8.
[37] O'Brien TA, Kluger R, Pike DC, Gennis RB. Phosphonate analogues of pyruvate. Probes of substrate binding to pyruvate oxidase and other thiamin pyrophosphate-dependent decarboxylases. Biochim Biophys Acta 1980;613:10–7.
[38] Bunik VI, Buneeva OA, Gomazkova VS. Change in alpha-ketoglutarate dehydrogenase cooperative properties due to dihydrolipoate and NADH. FEBS Lett 1990;269:252–4.
[39] Kovina MV, Kochetov GA. Cooperativity and flexibility of active sites in homodimeric transketolase. FEBS Lett 1998;440(1–2):81–4.
[40] Ciszak EM, Korotchkina LG, Dominiak PM, Sidhu S, Patel MS. Structural basis for flip-flop action of thiamin pyrophosphate-dependent enzymes revealed by human pyruvate dehydrogenase. Biol Chem 2003;278: 21240–6.
[41] Frank RA, Titman CM, Pratap JV, Luisi BF, Perham RN. A molecular switch and proton wire synchronize the active sites in thiamine enzymes. Science 2004;306:872–6.
[42] Nemeria N, Baykal A, Joseph E, Zhang S, Yan Y, Furey W, et al. Tetrahedral intermediates in thiamin diphosphate-dependent decarboxylations exist as a 1′,4′-imino tautomeric form of the coenzyme, unlike the Michaelis complex or the free coenzyme. Biochemistry 2004;43:6565–75.
[43] Varfolomeev SD. Enzyme inactivation in the reaction process. Regulatory role. Biokhimiia (Russian) 1984;49:723–35.
[44] Sud'ina GF, Kobel'kov GM, Varfolomeev SD. The macrokinetic behavior of an enzymatic system with an enzyme inactivated in the reaction. Biotechnol Bioeng 1987;29:625–32.
[45] Frank RAW, Kay KWM, Hirst J, Luisi BF. Off-pathway, oxygen-dependent thiamine radical in the Krebs cycle. J Am Chem Soc 2008;130:1662–8.
[46] Kahlert S, Zündorf G, Reiser G. Glutamate-mediated influx of extracellular Ca2+ is coupled with reactive oxygen species generation in cultured hippocampal neurons but not in astrocytes. Neurosci Res 2005;79:262–71.
[47] Kumar MJ, Nicholls DG, Andersen JK. Oxidative alpha-ketoglutarate dehydrogenase inhibition via subtle elevations in monoamine oxidase B levels results in loss of spare respiratory capacity: implications for Parkinson's disease. J Biol Chem 2003;278:46432–9.